1   **New evidence for the age and palaeoecology of the Knysna Formation, South Africa**

2   Andrew S Carr[1], Adam Dunajko[2], Arnoud Boom[1], Mark D Bateman[2], Peter J Holmes[3],

3   Juan-Carlos Berrio[1]

4   Corresponding author: A.S. Carr, asc18@le.ac.uk

5

6   1 Department of Geography, University of Leicester, UK: ab269@le.ac.uk; jcb34@le.ac.uk

7   2 Sheffield Centre for International Drylands Research, Department of Geography, University of

8   Sheffield, UK: m.d.bateman@shef.ac.uk; ggp07acd@shef.ac.uk

9   3 Department of Geography, University of the Free State, South Africa: holmespj@ufs.ac.za

10
11   **Abstract**
12   The existence of lignitic deposits (Knysna Formation) on the South African south coast, near to the

13   town of Knysna has been recognised for more than a century. However, a combination of limited

14   study and few natural exposures has meant that the age and stratigraphic position of the Knysna

15   Formation are unclear, despite its potential as a palaeoenvironmental archive. We present a new

16   suite of chronological, geochemical and palynological data obtained from a recently identified lignite

17   exposure in this area. The lignite pollen assemblage is dominated by palms (Arecaceae), which are

18   now locally extinct, and contains additional palynomorphs of tropical affinity, along with (moist-

19   temperate) *Podocarpus*-type pollen, grasses, and herbaceous pollen types (e.g. *Cliffortia*-type,

20   Asteraceae). Overall, the assemblage shows some commonalities with the Miocene Elandsfontein

21   Formation in the Western Cape. The lignites are dominated by a diverse range of higher plant

22   biomarkers, including abundant leaf wax lipids, as well as lignin monomers and leaf cuticle-derived

23   macromolecular organic matter. All strongly indicate a terrestrial depositional setting, perhaps akin

24   to contemporary palm swamps. A number of sesquiterpenoids imply the presence of gymnosperms,

25   supporting observations from the pollen data and previously reported macro-fossil finds.

26   The application of isothermal thermoluminescence techniques to coversands overlying the lignite

27   produced a minimum age of 1.7 Ma. Additional clues as to the likely age of the lignite are provided

28   by compound-specific stable carbon isotope analyses of the leaf wax lipids. These are approximately

29   8 ‰ enriched relative to typical C_3 vegetation leaf waxes, and imply a potential contribution from C_4

30   vegetation. From this, an age post-dating the Oligocene may be inferred, and in conjunction with the

31   site's geomorphic setting, an age post dating the middle Miocene is considered plausible. This is

32   markedly younger than previous (Eocene) age estimates for the Knynsa Formation.

33

34   Keywords: Neogene, pollen, biomarker, luminescence, stable isotope

35

36   **Introduction**

37   Due to its progressive aridification and predominantly erosive landscape history

38   (Partridge and Maud, 1987) southern Africa suffers from a paucity of palaeoecological

39   evidence. The Neogene palaeoecology of the southern African flora is however of great

40   significance and relevant to wider questions concerning patterns of floral dispersal and

41   diversification (Coetzee, 1983; Linder, 2003), the causes and effects of the Late Neogene

42   aridification of southern Africa, and the emergence of C_4 grasslands (Ségelan et al., 2007).

43   The occurrence of organic-rich sediments ("lignites") near to Knysna on the southern Cape

44   coast has been known of for more than a century (Phillips, 1927 and references therein).

45   These are now formally recognised as the Knysna Formation (Jacobs 1992), and comprise

46   sands, fine-grained muddy lignitic sands and lignites up to 30 m thick. Their relative

47   antiquity and palaeoecological significance were easily recognised (Phillips, 1927; Du Toit,

48   1956). Subsequently, Thiergart et al. (1963) and Coetzee et al. (1983) reported palynological

49   assemblages significantly different from the region's contemporary vegetation. These

50   studies revealed the presence of extant temperate forest vegetation (e.g. *Podocarpus sp.*,

51   *Widdringtonia cupressoides*), the absence of a number of common contemporary

52   palynomorphs (e.g. Ericaceae), and the presence of locally extinct flora (e.g. *Nypa*-type
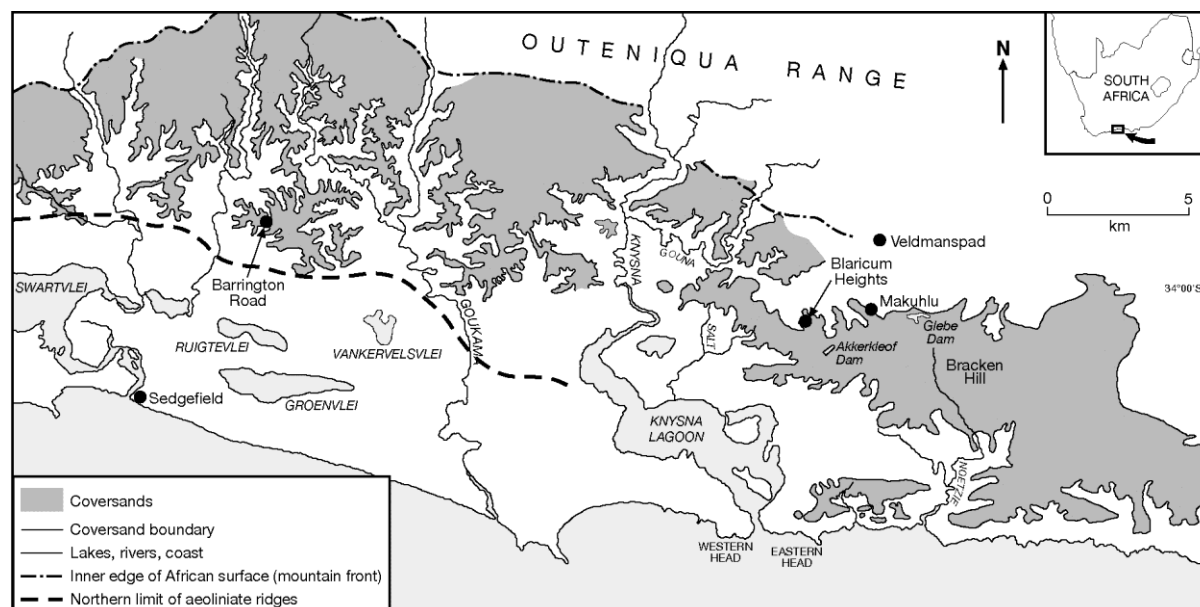
53   palm).

54   The extent, age and stratigraphic relationships between exposures of the Knysna

55   Formation remain unclear, and detailed information such as sample site location has often

56   been lacking in previous reports (e.g. Helgren and Butzer, 1977; Coetzee et al., 1983;

57   Thwaites and Jacobs, 1987). The limited available exposure and borehole data indicate that

58   all deposits are concentrated in the Veldmanspad and Brakenhill areas on a platform at

59   altitudes more than 200 m above modern sea-level (**Figure 1**; Jacobs, 1992). This landscape

60   setting alone implies an antiquity considerably greater than the Quaternary aged dunes and

61   wetlands immediately seawards (Holmes et al., 2007). Age estimates based on palynological

62   evidence (Coetzee et al., 1983) or landscape setting/stratigraphic relationships (Butzer and

63   Helgren 1972; Helgren and Butzer 1977; Thwaites and Jacobs, 1987; Marker and Holmes,

64   2002; Holmes et al., 2007) are disparate, encompassing a range between the Eocene and

65   the Miocene.

66   In the course of recent investigations into the origin and distribution of the Knysna

67   coversands, Holmes et al (2007) reported a 2-3 m thick sandy lignite deposit beneath a 15 m

68   sequence of aeolian coversands at Makhulu Quarry, c. 4 km southeast of Veldmanspad

69   (**Figures 1 and 2**). Optically stimulated luminescence (OSL) dating of the coversands

70   produced a minimum age of > 500 ka, but the underlying lignite was not investigated. The

71   aims of the present paper are:

72   1. Following initial attempts at OSL dating (Holmes et al., 2007), to reassess the age of

73   the coversands at Makhulu Quarry using recently developed isothermal

74   thermoluminescence (ITL) techniques. (Choi et al., 2006; Jain et al., 2007;

75   Vandenberghe et al., 2009).

76   2. To analyse the organic geochemistry and palaeoecology of the lignite exposed at

77   Makhulu   in   order   to   infer   its   likely   depositional   context   and

78   palaeoenvironment/palaeoecology.

79   3. To set the palaeoecological data in the context of palynological (Cole and Roberts,

80   1996; Scott, 1995) and palaeoecological (Hopley et al., 2007; Ségelan et al., 2007)

81   evidence for southern African flora.

82

83   **Figure 1**: Site locations in the Wilderness-Knysna region shown in relation to the mapped coversand
84   distribution (modified from Marker and Holmes, 2002). The broad locations of previous lignite
85   exposures (Brakenhill and Veldmanspad) are also shown.

86

87

88   ***Site description and stratigraphic setting***

89   Samples were obtained from Makhulu Quarry in 2004 (34°00'48"S 23°06'26"E;
90   altitude 220 m above modern sea-level [amsl]) which lies northeast of Knysna, and close to
91   the northern limits of the Knysna coversands mapped by Marker and Holmes (2002). The
92   stratigraphy of the site (which since sampling has been fully excavated) is shown in **Figure 2**.
93   The site lies within a hollow in the underlying Peninsula Formation (Table Mountain Group)
94   bedrock topography, which probably accounts for the enhanced thickness of the sand in this
95   location (Holmes et al., 2007). Up to 3 m of sandy lignites unconformably overlie the
96   Peninsula Formation quartzites and are themselves overlain by up to 15 m of weathered
97   and ferrugenised coversand deposits. Holmes et al. (2007) considered this the southern
98   Cape coversand type site and provided a detailed description of the coversand properties.
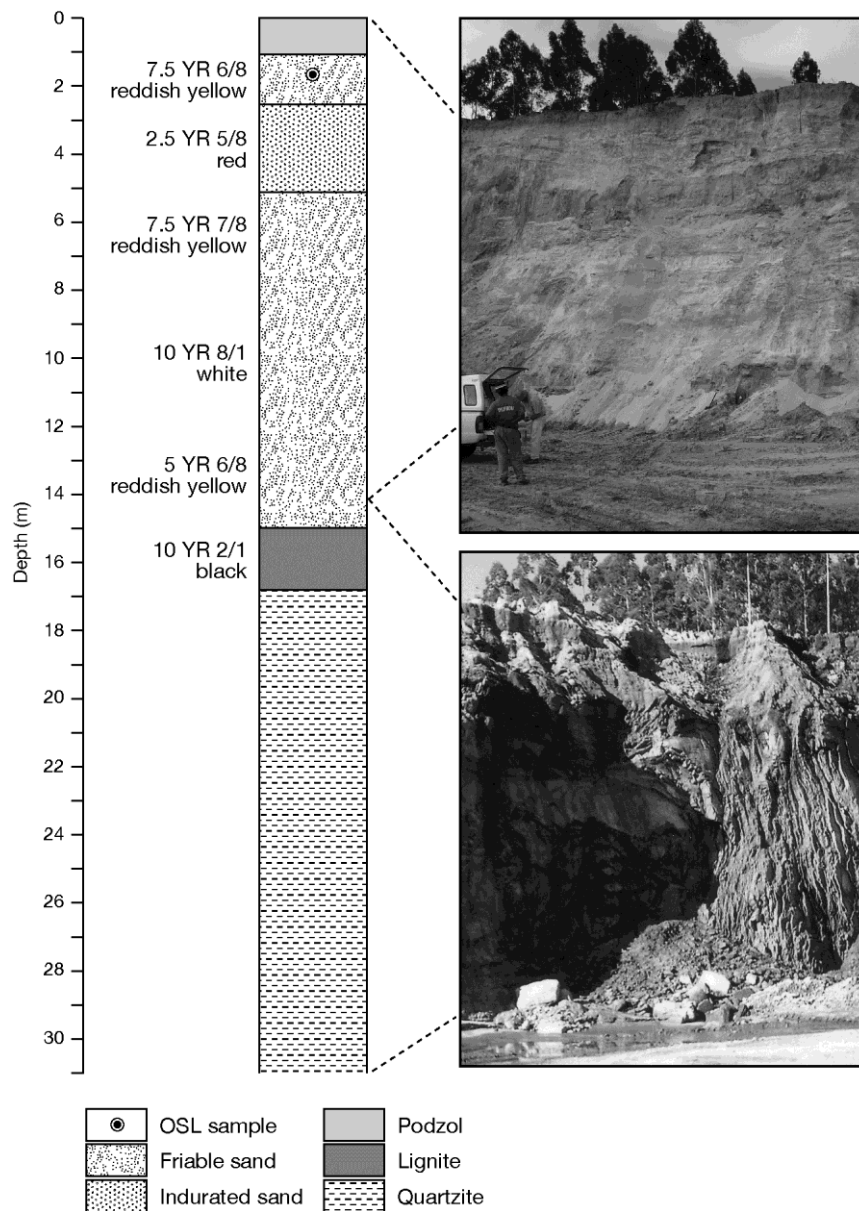
4

99

100

101

102

103 **Figure 2**: Site stratigraphy and photographs of Makhulu Quarry (in 2004). The location of the OSL
104 sample reported by Holmes et al., (2007) and re-evaluated in this study is shown. Note in upper
105 photograph the laterisation of the coversands (at c. 3-5 m depth) and in the lower photograph the
106 lignite/coversand contact.

107

108

109   ***Geochronology***

110   Optically stimulated luminescence (OSL) of quartz has been widely used in the

111   southern Cape to date mid to late-Pleistocene marine and aeolian sediment (e.g. Bateman

112   et al., 2004). The fundamental principle is that buried quartz acts as a dosimeter, storing up

113   trapped electrons in its crystal lattice in proportion to the natural (geological) radioactivity

114   in the environment (Aitken 1985). If buried for sufficient time quartz grains become

115   'saturated' (lattice cannot accommodate additional free electrons), which constrains the

116   upper limit of the technique. The time to saturation is largely a function of background

117   radioactivity and in low radiation environments reliable OSL ages approaching 500 ka have

118   been determined (Banerjee et al., 2003). Holmes et al. (2007) found that the coversands in

119   the Makhulu Quarry and the nearby Blaricum Heights site (**Figure 1**) were saturated using

120   standard OSL techniques and obtained minimum ages of >500 ka and >300 ka respectively

121   (**Figure 2**).

122   In this study we re-analyse one of the Makhulu samples reported by Holmes et al.

123   (2007), using an isothermal thermoluminescence (ITL) dating approach which seeks to

124   overcome the saturation issues previously encountered (Choi et al., 2006). While most OSL

125   dating relies on measuring electrons immediately evicted on optical stimulation (the 'fast

126   component' of the luminescence signal; Wintle and Murray, 2006), quartz grains also emit a

127   thermoluminescence (TL) signal upon heating, with peaks at 325°C and 375°C (Aitken, 1985).

128   New ITL dating protocols utilise a single aliquot regenerative dose (SAR) protocol akin to

129   standard OSL dating, but measure only the signal emitted from the 325°C TL peak, which is

130   known to be bleached by visible light (Franklin, 1997). Crucially, this signal saturates at much

131   higher doses than the OSL fast component. For instance, Jain et al. (2005) recorded a near

132   order of magnitude increase in the saturation dose of quartz grains using ITL compared to

133   OSL. There is thus potential for ITL to be used to date sediments beyond the range of

134   conventional OSL dating, which would be of significance given the extensive Neogene

135   marine and aeolian deposits along the Western Cape coastline.

136

137   *Methods*

138   Luminescence sampling, quartz sample extraction and dose rate determinations

139   followed Holmes et al. (2007). All luminescence measurements were carried out on a Risø

140   luminescence reader using 9.6 mm diameter aliquots with luminescence signals detected

141   through a Hoya U340 filter. Previous studies have employed a range of temperatures for

142   both the ITL stimulation and the sample preheat (Choi et al., 2006; Buylaert et al., 2006; and

143   Huot et al., 2006). To establish the applicability of ITL to the deposits in this study the

144   protocol was first tested using a coversand sample (Shfd08191 from Barrington Road, 33°

145   59'13 S, 22° 51'08 E; 90 m amsl; **Figure 1**) which was within the range of the standard SAR

146   OSL approach (equivalent dose of c. 240 Gy). For this sample SAR OSL equivalent doses (D_e)

147   were determined following Murray and Wintle (2000), with ITL D_e values at both 300°C and

148   310°C determined for a range of preheat temperatures (240°C to 270°C in 10°C increments;

149   Choi et al., 2006; **Table 1**).   For sample Shfd08191 ITL D_es obtained at 310°C were

150   consistently closer to the OSL D_e than those obtained using ITL at 300°C (**Figure 3**). The

151   measurements at 310°C also produce a D_e plateau at preheats of 260°C and below. Based

152   on these results, an ITL stimulation temperature of 310°C and a preheat temperature of

153   260°C were selected for full ITL measurement of the sample. Growth curves were fitted with

154   a saturating exponential function (**Figure 4**). For the purposes of subsequent age estimation

155   all aliquots with a recycling ratio outside 1 ± 0.2 were rejected prior to D_e calculation.

156   Sunlight bleaching of the ITL signal was tested by exposing seven aliquots of the Makhulu

157   Quarry sample (Shfd04287) to (UK) daylight for 1 week. A residual ITL D_e of 4.73 ± 0.34 Gy

158   (n=7) was determined (**Figure 5a**; **Table 2)**, which given the magnitude of the sample

159   equivalent doses, was considered small enough to be of negligible significance. For the

160   Makhulu sample (Shfd04287) 24 aliquots were measured using an ITL stimulation

161   temperature of 300°C and a preheat temperature of 260°C (determined experimentally in

162   an identical manner to the above). **Table 2** shows the finalised OSL and ITL D_e values used

163   for age calculation reported with 1 sigma uncertainties.

164

165   *Results*

166   For Shfd08191 (Barrington Road), the mean D_e values from the OSL and ITL

167   approaches are broadly similar and are within 1 standard deviation of each other (OSL D_e =

168   242 ± 30; ITL D_e = 295 ± 50; **Figure 5**). The slightly higher mean D_e for ITL results may reflect

169   a signal contribution from TL traps incompletely bleached by sunlight prior to burial (**Figures**

170   **5b and 5c)**.   More significantly in the context of the coversands, while the OSL growth

171   curves typically saturate at 350 ± 50 Gy (**Figure 4a),** the ITL growth curves grow beyond 550

172   Gy (**Figure 4b)**. As such, and given the favourable comparison of ITL to OSL data, it is

173   inferred that the ITL procedure can provide new age constraints on Knysna coversand

174   material beyond those presented by Holmes et al (2007). ITL measurements on the

175   Makhulu quarry sample (Shfd04287) reveal the naturally acquired ITL signal to be very large

176   (**Figure 6**) and for two aliquots this was significantly higher than the maximum administered

177   laboratory dose, which prevented interpolation. These aliquots were rejected from

178   subsequent analyses. The remaining aliquots were fitted with saturating exponential growth

179   curves (**Figure 6b**), of which eight were in saturation (on average the Makhulu sample

180   growth curves saturated at 1390 ± 490 Gy). The remaining 10 aliquots, for which a D_e could

181   be estimated, produced a mean D_e of 806 ± 58 Gy **(Figure 5d)**, from which an age of 1.7 ±

182   0.14 Ma was derived **(Table 2).** With 40% of the aliquots measured by ITL in saturation this

183   is clearly a minimum D_e and thus, age estimate for the coversand (and lignite) at this site. It

184   is however more than triple the minimum age obtained via SAR OSL (Holmes et al., 2007)

185   and it suggests a pre-Quaternary antiquity for both the coversands and the underlying
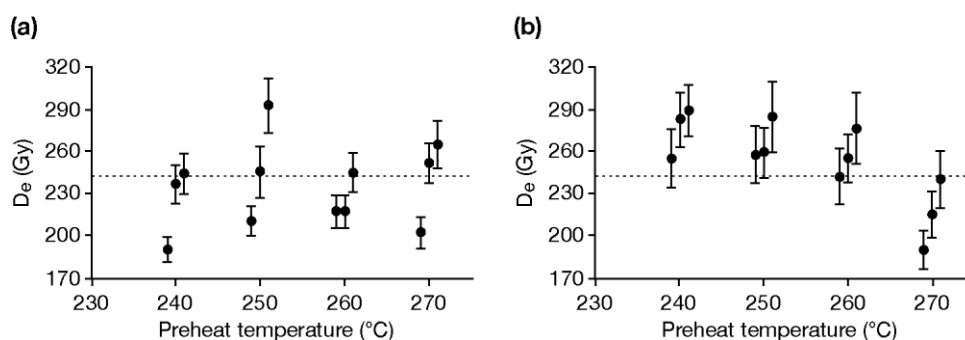
186   lignite.

188   **Figure 3**: Preheat plateau tests undertaken to establish the optimum ITL stimulation and preheat

189   temperatures for sample Shfd08191: (a) ITL at 300°C (b) ITL at 310°C. Dashed line shows D_e of

190   sample established using conventional SAR OSL. Note for clarity aliquots measured at the same
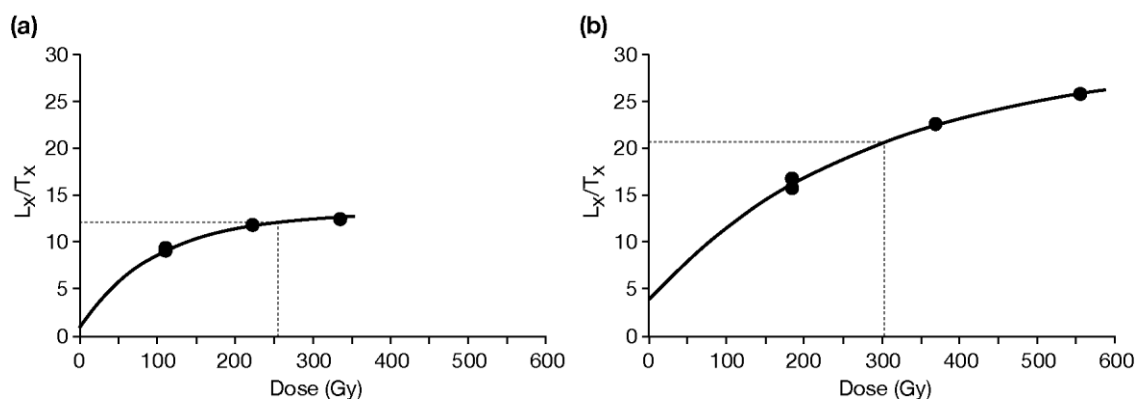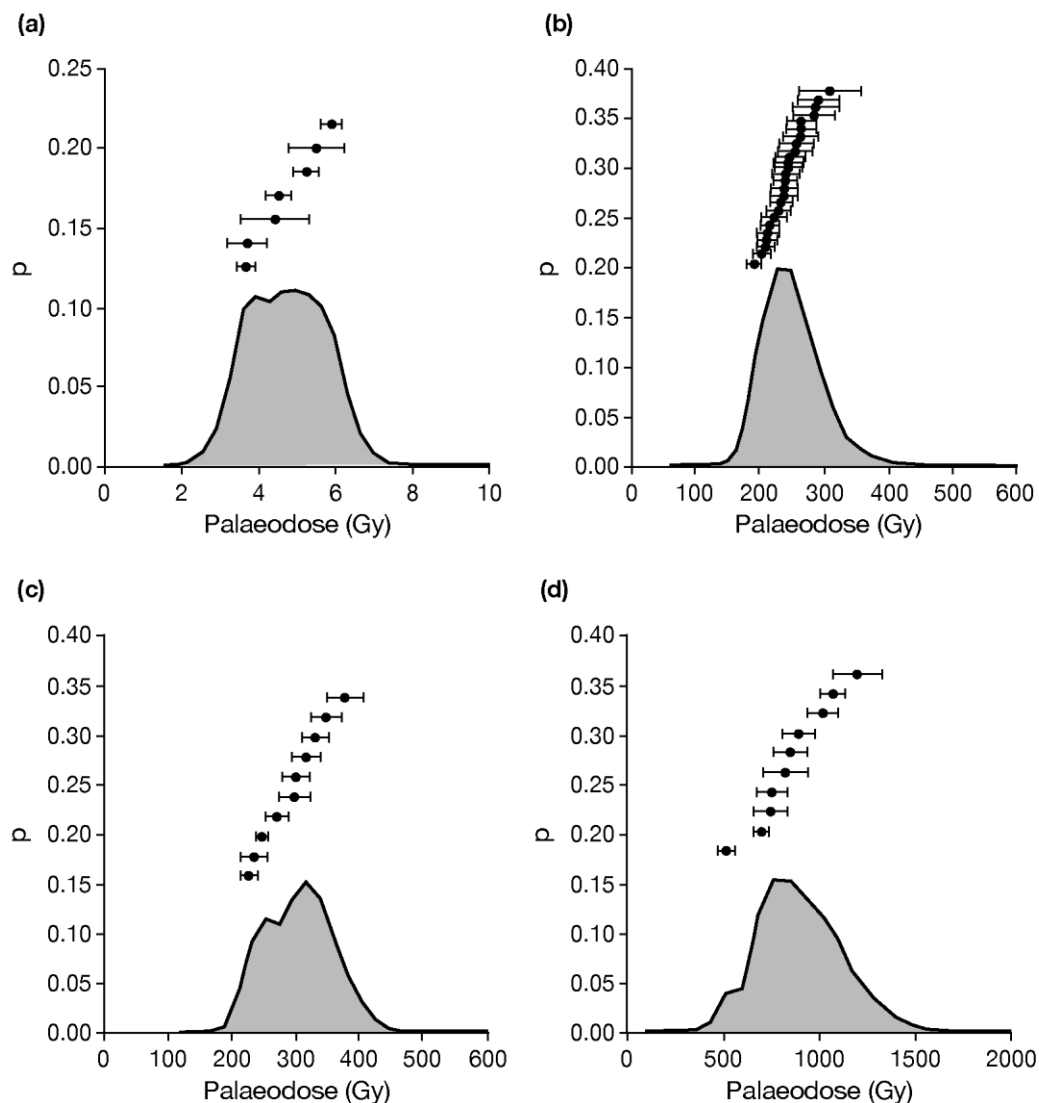
191   preheat temperatures are slightly offset.

192

194   **Figure 4**: Example growth curves for individual aliquots from sample Shfd08191: (a) OSL and (b) ITL

195

9

196

197

Figure 5: D_e distributions of samples measured (a) ITL of sample Shfd04287 after exposure to daylight for seven days. Average D_e = 4.73 ± 0.34 Gy (b) OSL D_e distribution for sample Shfd08191 from Barrington Road (c) ITL D_e distribution for sample Shfd08191 from Barrington Road (d) ITL D_e distribution for sample Shfd04287 from Makhulu Quarry.
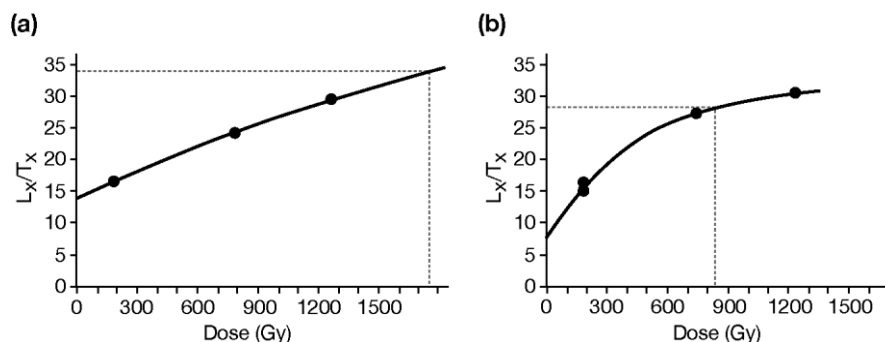
202

203

205   **Figure 6:** Example ITL growth curves for sample Shfd04287

206

207   ***Organic geochemistry***

208   The last two decades have seen the rapid development of palaeoecological and

209   palaeoenvironmental approaches using biomarkers (see Eglinton and Eglinton, 2008 for an

210   overview). Suites of biomarkers within organic matter reflect the composition of the

211   original inputs to a sample (e.g. local ecology) and the effects of subsequent microbial and

212   diagenetic degradation. In this study we have applied solvent-extractable lipid analyses, and

213   pyrolysis-GC/MS (py-GC/MS) analyses to the Makhulu lignite. The pyrolysis technique

214   provides insights into the origin and diagenetic alteration of insoluble macromolecular

215   organic matter (e.g. lignin) within a sample. Using these techniques we assess the Makhulu

216   depositional setting, the extent of organic matter preservation/diagenesis, and the

217   palaeoenvironmental setting of the site. These new data are interpreted in light of

218   accompanying palynological analyses, and potential points of comparison for future lignite

219   finds are noted.

220

221   *Methods*

222   The sampled lignite was freeze dried and homogenised prior to analysis. Total C and

223   N data were measured using a SerCon ANCA GSL elemental analyser connected to a SerCon

11

224   Hydra 20-20 continuous flow isotope ratio mass spectrometer (cf-IR-MS). Solvent-

225   extractable lipid biomarkers were extracted using a series of solvents of progressively

226   decreasing polarity (methanol; dichloromethane (DCM); hexane). Extracts were eluted over

227   an Al_2O_3 column to derive apolar and polar fractions. The polar fractions were derivatized

228   using bis(trimethylsilyl)trifluoroacetamide (BSTFA) for 1 hour at $60°C$ prior to analysis.

229   GC/MS analyses were carried out on a Perkin Elmer Clarus 500 GC-MS system fitted with a

230   CP-Sil 5CB MS column (30 m x 0.25 mm). Compounds were identified on the basis of their

231   retention times and mass spectra. Compound specific stable isotope analyses were

232   conducted on the apolar solvent fraction using an Agilent 6890N gas chromatograph

233   equipped with a combustion reactor, interfaced to a SerCon GC-CP which was connected to

234   the Hydra 20-20 cf-IR-MS. Results are presented as an average of three solvent injections

235   with accompanying standard deviations (better than 0.5 ‰ for all reported compounds).

236   Pyrolysis GC/MS was conducted using a CDS 1000 pyroprobe coupled to the Perkin Elmer

237   Clarus 500 GC-MS system. Approximately 0.5 mg of sample was encapsulated in a quartz

238   tube and held in place with quartz wool. The sample was then pyrolysed at $610°C$ for 15

239   seconds. Measurements were conducted on an untreated sample, as well as the residue

240   remaining following saponification (reflux in KOH and methanol). This process hydrolyses

241   certain chemical bonds (ester bonds), and assists in characterising the original nature of the

242   macromolecular organic matter (some macromolecules will be resistant to this process).

243

244   *Results*

245   The total organic carbon (TOC), total nitrogen (TN) and $\delta^{13}C_{TOC}$ of the lignite are

246   shown in **Table 3**. The TOC/TN ratio is very high (45) and suggestive of organic matter

247   dominated by terrestrial / higher plant-derived organic matter, as opposed to algal-rich

248   lacustrine organic matter, which typically exhibits lower TOC/TN ratios (4-10; Meyers and

249   Lallier-Vergès, 1999). These data are consistent with Phillip's (1927) observations of well-

250   preserved plant macro-fossils within the lignite.
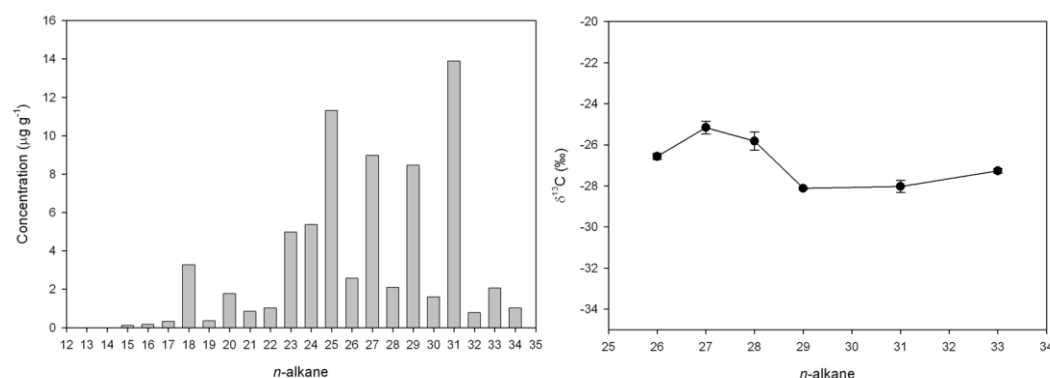

251

252

253   **Figure 7**: The *n*-alkane distribution (absolute concentrations) and *n*-alkane δ^{13}C values obtained from

254   the apolar solvent extract. End member *n*-alkane δ^{13}C values for C_3 and C_4 vegetation are typically -

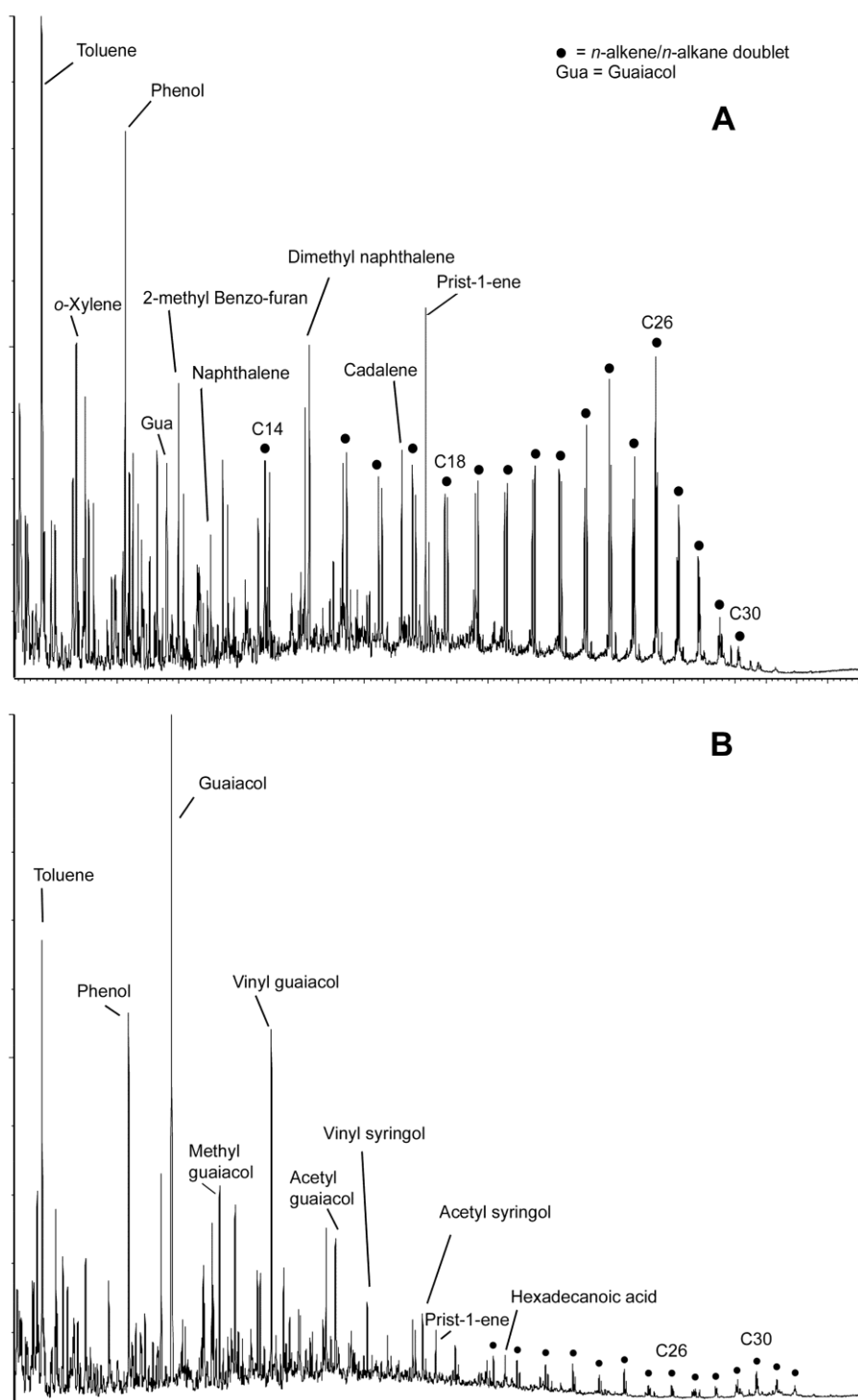255   20‰ and -35‰ respectively (Boom et al., 2002).

256

257

258

Figure 8: Pyrograms (total ion current) of (A) Knysna lignite and (B) contemporary wetland sediments from Still Bay area. Peak heights are normalised to the highest peak in each sample. The GC programme comprised an initial temperature of 40°C for 1.8 minutes, ramped to a final temperature of 310°C at 4°C min^{-1} which was held for 20 minutes. Major peaks are labelled (with chain length indicated where appropriate) with selected structures shown

14

265   The extractable lipids comprise a homologous series of *n*-alkanes, pentacyclic

266   triterpenoids and des-A-triterpenoids (des-A-Lupane and Olean-12-ene) in the apolar

267   extract, and a homologous series of *n*-alkanols (C_{16}-C_{28}), as well as the compounds β-amyrin

268   (olean-12-en-3β-ol), α-amyrin and friedelan-3-one in the polar extracts. The *n*-alkane

269   distribution (**Figure 7**) is bi-modal, peaking at C_{25} and C_{31}. *n*-alkanes in the range C_{27} to C_{33}

270   are generally considered to derive from higher plant epicuticular leaf waxes (Eglinton and

271   Hamilton, 1967) and as observed here, are characterised by odd over even chain length

272   dominance (expressed as the carbon preference index; 'CPI'). A secondary peak is seen

273   within the mid chain length *n*-alkanes (C_{21} to C_{25}). These shorter odd chain length *n*-alkanes

274   (C_{23} and C_{25}) have been associated with submerged or floating plants, rather than terrestrial

275   plants or emergent macrophytes such as *Typha* and *Phragmites* (Ficken et al., 2000). This

276   distinction forms the basis of the P_{aq} index, which is used to assess the relative significance

277   of submerged, emergent or terrestrial vegetation (Ficken et al., 2000). The P_{aq} value of 0.42

278   for the Makhulu lignite is transitional between terrestrial vegetation / emergent

279   macrophytes (typically 0.1-0.4) and submerged / floating plant matter (typically 0.4 – 1.0).

280   This interpretation implies the presence of some floating/aquatic vegetation, and

281   potentially a partially open water environment.

282   A number of sesquiterpenoids, notably caladene, and calamenene were detected

283   (Bechtel et al., 2002; Stefanova et al., 2005). These are typical coal biomarkers and are

284   common constituents of resins from the Podocarpaceae, Cupressaceae and Pinaceae

285   families (Otto et al., 2005). In this case the sesquiterpendoids extracted from Makhulu

286   cannot be associated with any individual plant family, but their occurrence strongly suggests

287   the presence of gymnosperm vegetation in the site vicinity. Similarly, although most lipid

288   biomarkers are indicative of a higher plant (angiosperm) origin, none can be used as

289   chemotaxonomic indicators (e.g. Pancost and Boot, 2004).

290   The other major constituents of the lipid extracts are hopanes, and their diagenetic

291   isomers, moretanes, which are typically derived from bacterial activity and are common in

292   many lignite deposits (e.g. Bechtel et al., 2002; Bechtel et al., 2003; Otto et al., 2005). Here

293   they are dominated by 17β-22,29,30 trisnorhopane and 17β 21α-homomoretane. Hop-

294   17(21)-ene is also present. Diagenetically immature samples are dominated by hopanes in

295   the (biological) 17β 21β isomeric configuration (Pancost et al., 2007) and the presence of

296   some hopanes in the 17α 21β configuration reveals the occurrence of minor diagenetic

297   alteration.

298   The lignite pyrolysate (i.e. solvent insoluble OM) is shown in **Figure 8A**, with surface

299   sediment from a contemporary southern Cape wetland for comparison (**Figure 8B**). The

300   Makhulu lignite is dominated by aromatic and aliphatic compounds, with the latter, which

301   comprise a series of long chain (C_8 to C_{32}) *n*-alkene/*n*-alkane doublets, accounting for 52% of

302   the total ion current (TIC) and peaking at chain lengths of C_{10}-C_{15}, and C_{21} to C_{26}. These

303   aliphatics are substantially more significant in the lignite than in the modern sample (< 19 %

304   of TIC). They may be derived from a range of potential biological sources, including cutin, a

305   biopolymer derived from leaf cuticles, which may be preserved in samples of a geological

306   antiquity (Logan et al. 1993). Other potential sources include cutan, a resistant biopolymer

307   derived from certain plant cuticles (Nip et al., 1989; Boom et al., 2005), algaenan, which is

308   derived from some freshwater algae (Blokker et al., 1998), and geo-polymers formed post-

309   deposition (Yang et al., 2005; Gupta et al. 2007). The pyrolysate of the saponified residue

310   reveals a reduction in the significance of the doublets longer than C_{24}, implying the presence

311 of cutin monomers (Logan et al., 1993). A residual aliphatic signal remains, and given the

312 lack of evidence for algal organic matter in the sample (e.g. high TOC/TN ratio, the low

313 significance of short chain alkanes, and the absence of specific algal biomarkers) this most

314 likely represents a plant-derived macromolecule (e.g. cutan) and/or a post-depositional geo-

315 polymer. The former source is of interest given the isolation of cutan in the leaves of extant

316 *Podocarpus* sp. (Boom et al., 2005), and the occurrence of macro-remains of *Podocarpus* in

317 the Knysna Formation (Phillips, 1927). In conjunction, a number of lignin pyrolysis products

318 were identified, which are of a lower relative significance and diversity (0.8% TIC) than the

319 modern sample (c. 30% of TIC). This probably reflects the aerobic degradation of lignin. The

320 lignin monomers are dominated by guaiacol and degradation is implied by both the lack of

321 alkylated guaiacol lignin monomers and the trace amounts of (less resistant) sinapyl-derived

322 lignin monomers.

323

324 *Compound specific stable isotopes*

325 Inferring terrestrial palaeoenvironmenta from bulk stable isotope data in lacustrine

326 contexts may be complicated by the incorporation of biomass from multiple sources (Street-

327 Perrott et al., 2004). Due to their wide distribution within the atmosphere (Conte and

328 Weber, 2002) the isotopic signature of leaf wax lipids can provide useful insights into

329 *regional* palaeoecological conditions (Boom et al., 2002). The δ^{13}C values determined for the

330 C_{27} to C_{33} *n*-alkanes in the Makhulu lignite fall between -25 and -28 ‰ (weighted mean δ^{13}C

331 -27.0 ‰; **Figure 7 and Table 4**). The dominance of the C_{31} alkane and the depletion of the

332 C_{29} and C_{31} homologues are consistent with a leaf wax origin (Collister et al., 1994). These

17

333 isotopic ratios are substantially more enriched than leaf waxes derived from pure C$_3$

334 vegetation (typical δ^{13}C of -35 ‰; Collister et al., 1994; Boom et al., 2002).

335   Compound specific δ^{13}C measurements on the bacterially-derived hopanes (**Table 4**)

336 reveal slight enrichment (-20 and -25 ‰) relative to the bulk organic matter (-26.6 ‰). This

337 has been observed in both contemporary wetlands and Palaeogene lignites (Pancost et al.,

338 2007). The hopane δ^{13}C values do not indicate anaerobic conditions (*ibid*), which is

339 consistent with the py-GC/MS data for the (aerobic) degradation of lignin. Similarly, there is

340 no evidence for anaerobic methane oxidation (e.g. depleted hopane δ^{13}C values).

341

342

343

344 ***Palynological analysis***

345   Palynomorphs (**Figure 9 and Table 5**) are abundant in the Makhulu lignite,

346 but are often poorly preserved (8% were damaged or unidentifiable). From a count of 250

347 palynomorphs the sampled assemblage is dominated by palms (37 %). Poaceae (4.6 %,)

348 Cyperaceae (6.7 %) and *Podocarpus*-type pollen (3.8 %) are also frequently identified. The

349 palm (Arecaceae) pollen is mostly monosulcate in form, preventing easy associated with a

350 single family or subfamily (e.g. Harley and Baker, 2001). Pollen from typical *fynbos*

351 vegetation is mostly lacking (e.g. Ericaceae). One palynomorph closely resembling the

352 Rosaceae genus *Cliffortia* was identified, along with pollen resembling *Anthospermum*-type

353 (Rubiaceae) and two examples of a small tricolporate palynomorph akin to Grubbiaceae.

354 One triporate palynomorph with a triangular amb potentially represents Proteaceae.

355 Asteraceae pollen (2.9 %) of the Vernonia and Asteroideae types was identified (e.g. Scott,

356   1982; Skvarla et al., 2005). A number of palynomorphs were of unclear affinity, the most

357   common being a tetracolporate grain (6.7 %), resembling pollen from the family Sapotaceae

358   (**Figure 9**), and a tetraporate grain (5 %) resembling the pollen of *Symphonia* (Clusiaceae;

359   **Figure 9**). Pollen resembling the latter type has also been identified in Miocene sediments

360   from the Angola Basin (Partridge, 1978). In the contemporary tropics (South America, West

361   Africa, and Madagascar) this genus is often riparian or found within palm swamps (Ledru,

362   2001; Berrio et al., 2002). Along with palms, other pollen types of potential tropical affinity

363   include Malvaceae and Moraceae. Trilete and monolete spores were also common, and

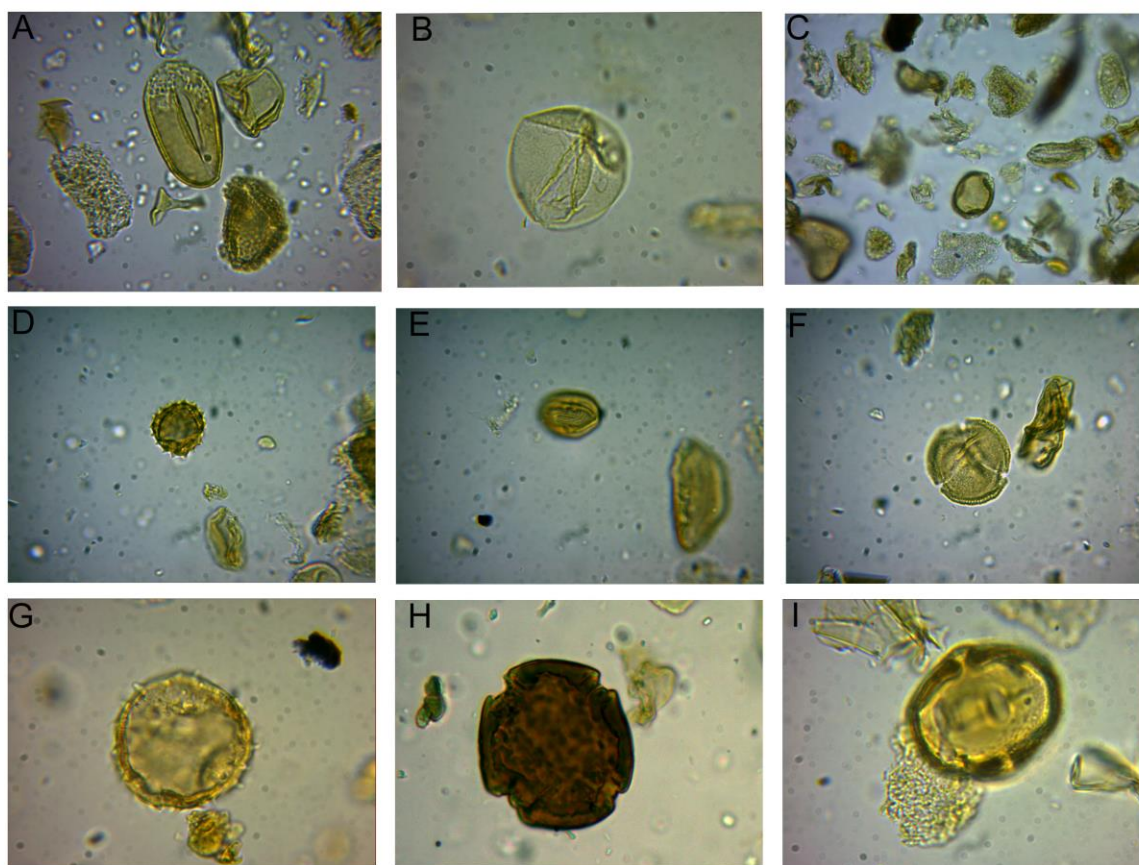364   comprised 3.8 % of the pollen spectrum.

365

366   **Figure 9**: Photograph montage of key pollen types identified within the sample A: Palm; B: Poaceae;
367   C: *Cliffortia*-type; D: Asteraceae; E: *Rhus*-type; F: Rubiaceae(?); G: Malvaceae; H: *Symphonia*-type; I
368   Tetracolporites (Sapotaceae).

19

369 ***Discussion and synthesis***

370 *Depositional setting*

371   Overall, the data imply that the lignite formed in a marshy environment surrounded

372 by significant emergent and riparian vegetation (e.g. Cyperaceae pollen). The biomarker

373 data and the bulk C/N ratios indicate little algal organic matter contribution to the lignite.

374 The pyrolysis data similarly imply that a substantial proportion of the macromolecular

375 organic matter is derived from terrestrial plants; notably leaf cuticles (cutin) and lignin

376 monomers. The presence of the sesquiterpenoids cadalene and calamenene in the lipid

377 extracts is strongly indicative of inputs from gynomsperm resins and is supported by the

378 presence of *Podocarpus* pollen. The biomarker data are therefore primarily indicative of

379 inputs from terrestrial/riparian plant-derived organic matter, although the P_{aq} parameter

380 implies the presence of some submerged or aquatic plants. Such a terrestrial wetland

381 setting is consistent with some interpretations of the Knysna Formation (Coetzee et al.,

382 1983). This was not a strongly anoxic environment, nor is there evidence for marine-derived

383 organic matter (c.f. Volkman et al., 2008). This does not rule out wetland formation

384 associated with high water tables during periods of high relative sea-level (*sensu* Cole and

385 Roberts 1996), but it is not strongly supportive of a back-barrier lagoon or estuarine setting.

386   The difficult terrain and limited exposure means that the stratigraphic relationship

387 between Makhulu and other reported lignite exposures in the Knysna region (i.e.

388 Veldmanspad and Brakenhill) is uncertain (Holmes et al., 2007). Such complexity serves to

389 highlight the need to document the biostratigraphic and palaeoecological evidence within

390 each lignite exposure. The maximum recorded altitude of the lignites is 320 m amsl

391 (Veldmanspad), with the Brakenhill lignites reportedly lying at c. 259 m amsl (Thwaites and

392 Jacobs, 1987) and Makhulu at 220 m amsl. Marker and Holmes (2002) noted the altitudinal

393 and spatial separation of the Knysna Formation deposits at Veldmanspad, Brakenhill and

394 Fisantshoek from the coversands, while Thwaites and Jacobs (1987) also suggested that

395 lignite deposits may represent spatially and temporally discrete deposits. This clearly has

396 implications for age-related and palaeoecological comparisons with the Makhulu lignite, but

397 it is hoped that the palynological and geochemical data presented here will provide useful

398 points of comparison.

399

400 *Age estimates*

401   The ITL analyses on the overlying coversand provide the first numerical age

402 constraints on the Knysna Formation. While the data presented by Holmes et al (2007)

403 demonstrated an age pre-dating the Late Pleistocene, the application of ITL pushes this

404 minimum age back to > 1.7 Ma. The gradational boundary between the coversand and

405 lignite units suggests that they were deposited at a similar time. The ITL result therefore

406 implies that the Makhulu lignite may pre-date the Quaternary Period. The ITL age of 362 ±

407 35 ka for the Barrington Road coversand (Shfd08191) is similar to the minimum ages

408 reported by Holmes et al. (2007) for the Blaricum Heights coversands. Both sites are clearly

409 within the coversand sheet, but their relationship with Makhulu is unclear. Their essentially

410 mid-Pleistocene ages, in conjunction with the new Makhulu ITL data, do however support

411 the previous inference that parts of the coversand system have been reworked during the

412 Quaternary (Holmes et al., 2007).

413   The compound-specific stable isotope data also provide potential constraints on the

414 likely age of the Makhulu lignite. The weighted mean (C_{27}-C_{31}) *n*-alkane $\delta^{13}C$ value of -27 ‰

415   indicates inputs from non-C_3 vegetation sources; the end member $\delta^{13}C$ values for C_3 and C_4

416   plant leaf waxes being -35 and -20 ‰ respectively (Boom et al., 2002). Presently, in

417   southern Africa C_4 photosynthesis is abundant in both grasses (Poaceae) and sedges (Vogel

418   et al., 1978; Stock et al., 2004). Compound-specific stable isotope data of this type have

419   previously been used to track the emergence of C_4 grasses during the Neogene (Freeman

420   and Calarusso, 2001). A simple two part mixing model with the above-noted end members

421   implies a C_4 contribution to the leaf wax signal as high as 53 %. This approach however

422   assumes no input from CAM (crassulacean acid metabolism) vegetation, which exhibit highly

423   variable leaf wax $\delta^{13}C$ values (ranging between -21 to -29 ‰; Collister et al., 1994; Bi et al,

424   2005), and it also assumes that there is little inter-species variability in the ^{13}C offset

425   between whole plant tissue and leaf wax *n*-alkanes (Freeman and Calarusso, 2001).

426   There is currently little published data on CAM plant leaf wax $\delta^{13}C$ variability, making

427   this issue difficult to resolve. This result is however intriguing. Presently CAM plants are

428   found in the southern Cape area, while grass pollen, which can dominate Quaternary and

429   contemporary pollen spectra, is a relatively minor component of the Makhulu pollen

430   spectrum. The efficacious dispersal of leaf waxes in the atmosphere implies that the *n*-

431   alkane $\delta^{13}C$ integrates a vegetation signal from a substantial land area (Conte and Weber,

432   2002; Rommerskirchen et al., 2003), and in the absence of other evidence at present, a C_4

433   contribution of some size represents a parsimonious interpretation. Assuming a non-

434   negligible contribution of C_4 vegetation, an age close to or post-dating the expansion of C_4

435   grasses in the Late Miocene (c. 10 Ma; Cerling et al., 1993; Freeman and Calarusso, 2001)

436   might be inferred, with an upper age further constrained by genetic evidence for the origins

437   of C_4 vegetation. Given that this origin probably lies in the Oligocene (Tipple and Pagani,

438 2007), and for C_4 Cyperaceae, in the Miocene (Besnard et al., 2009), even a small C_4

439 contribution casts doubt on an Eocene age estimate (cf. Coetzee et al., 1983; Thwaites and

440 Jacobs, 1987). In southern Africa Ségalen et al. (2007) concluded that the C_4 expansion

441 occurred as late as 4-5 Ma; an estimate supported by $\delta^{13}C$ data from speleothems in the

442 Makapansgat Valley in the summer rainfall zone (Hopley et al., 2007).

443   The Makhulu site lies on a coastal platform thought to have formed after a phase of

444 uplift in the early-mid Miocene (Partridge and Maud, 1987). The early to middle Miocene

445 was a phase of global warmth and associated high eustatic sea-levels (Haq et al., 1987; John

446 et al., 2004; Tripati et al. 2009), representing a plausible origin for this surface. This setting is

447 not therefore inconsistent with a Miocene or younger age, as inferred from the n-alkane

448 $\delta^{13}C$ data. Given the current site altitude (220 m), a proposed phase of later Neogene uplift

449 (c. 150-200 m in the Pliocene; Partridge and Maud 1987) places the site close to sea-level,

450 the water table and a potential sediment source for the overlying coversands between the

451 late Miocene and early Pliocene (c. 10-5 Ma). Such an interpretation however ignores the

452 significant eustatic sea-level changes during this period (Haq et al., 1987; Le Roux, 1990;

453 John et al., 2004; Miller et al., 2005) and more recently Roberts and Brink (2002) have

454 argued for a stronger eustatic imprint on the Western Cape coastal record. However,

455 disentangling these eustatic and tectonic factors without additional data is clearly difficult

456 and beyond the scope of this paper.

457

458 *Regional palaeoecology*

459   The pollen preserved at Makhulu provides some indication of the local and regional

460 ecology. Palms are currently extinct in the southern and Western Cape, and along with the

461 presence of palynomorphs of possible tropical affinity (Malvaceae, Moraceae, Sapotaceae,

462 and *Symphonia*-type) the Makhulu data are suggestive of warmer and more humid

463 conditions than the present. Interestingly, given the efficacious dispersal of saccate pollen,

464 the proportion of *Podocarpus*-type does not suggest a dominant presence in local/regional

465 environment (see also Coetzee et al., 1983), which contrasts with Holocene pollen spectra in

466 this region (Martin, 1968). *Rhus*–type pollen is moderately-well dispersed (Scott, 1982), and

467 may have been present in the local environment. Asteraceae may represent a wide range of

468 southern African environments, but they are especially dominant in contemporary Karoo

469 and *fynbos* environments. We thus infer a wetland (Cyperaceae, Aponogetonaceae),

470 associated with a surrounding palm swamp or "gallery forest" vegetation community

471 (palms, *Symphonia*-type), which in turn was surrounded by a mixed vegetation community

472 comprising arboreal taxa (e.g. *Podocarpus* sp.), herbs (*Cliffortia*-type, *Anthospermum*-type)

473 and grasses. The proportion of grasses is relatively low compared to the contemporary

474 environment (Martin 1968), although these may be under-represented given the potentially

475 high proportion of the locally-derived pollen from the palm swap vegetation.

476   This assemblage differs from previous descriptions of palynomorph assemblages

477 from the Knysna Formation (Thiergart et al., 1963; Coetzee et al., 1983). A comparative

478 summary is shown in **table 5**. Key differences include the dominance of palm pollen at

479 Makhulu, which was either absent or tentatively identified (respectively) by Thiergart et al.

480 (1963) and Coetzee et al. (1983). An additional sample, apparently from the Veldmanspad

481 area, has been reported to contain high concentrations of palm pollen resembling

482 *Jubaeopsis* and *Nypa* (Helgren and Butzer, 1977; Scott, 1995). Pollen of the distinct *Nypa*

483 morphology was not identified at Makhulu. Van Zinderen Bakker (1984) reported palm

484   pollen in marine sediments as young as the Late Pliocene north of Namibia, while palm

485   pollen of the same monsulcate morphology as Makhulu Quarry has also been identified in

486   the Miocene Elandsfontein formation (Coetzee and Rogers, 1982). Asteraceae pollen, two

487   types of which were found in the Makhulu assemblage, has not been identified in previous

488   studies of the Knysna Formation. Other studies of the Knysna Formation have also reported

489   Proteaceae pollen (possibly identified at Makhulu) to be common, and grass pollen to be

490   present, but rare (Helgren and Butzer 1977; as at Makhulu). Given these apparent

491   differences in floral composition, the possibility that the Knysna Formation sites are

492   diachronous cannot be ruled out. It is currently difficult to evaluate this further given the

493   limited information on previous site locations and pollen assemblages.

494   Looking further afield, Coetzee (1983) interpreted proposed Miocene pollen spectra

495   from Noordhoek (Cape Town) and the Elandsfontein Formation near Langebaanweg

496   (Coetzee and Rogers, 1982) as indicative of mixed coniferous forests with tropical elements

497   and varying proportions of palms. The minimum age of the pollen assemblage at

498   Langebaanweg is constrained by overlying Varswater Formation (Franz-Odendaal et al.,

499   2002 and references therein) and contains substantial amounts of palm pollen, as well as

500   *Podocarpus*, *Widdringtonia*, Casuarinaceae, and Anacardiaceae. From the non-arboreal taxa,

501   Asteraceae, *Cliffortia*-type, Proteaceae, and (possibly) Thymelaeceae and *Stoebe*-type were

502   identified. At Noordhoek Asteraceae pollen was sparse or absent in the (presumed) early-

503   mid Miocene parts of the record (Coetzee, 1983). During the early Pliocene increased

504   abundances of Asteraceae pollen were associated with the loss of tropical pollen types;

505   notably the palms (*ibid*; Coetzee 1986).

506   Additional data pertaining to the Elandsfontein Formation were presented by Cole

507   and Roberts (1996). Here, samples from borehole LNV4 close to the Berg River contained

508   palynomorphs characteristic of *fynbos* vegetation (e.g. Proteaceae, *Passerina*-type,

509   *Anthospermum*-type), as well as Asteraceae (*Brachylaena*-type and undifferentiated) and

510   Poaceae pollen. The similarities were considered sufficient to warrant association with the

511   Langebaanweg record, although palm pollen was absent from the LNV4 samples. Scott

512   (1995) presented data for three samples from the Pliocene Varswater Formation and

513   identified a range of typical *fynbos* pollen types (*Cliffortia*-type, Restionaceae, Proteaceae,

514   and Ericaceae), along with Asteraceae and grass pollen. Palm pollen was only identified in

515   the deepest sample, which was considered transitional from the sub-tropical environments

516   of the Elandsfontein Formation.

517   Palaeogene (Eocene) age estimates for the Knysna Formation have been inferred on

518   the basis of the palynological data and notably, the absence of Ericaceae pollen (Thwaites

519   and Jacobs, 1987). It is notable that none of the Knysna Formation sites apparently contain

520   Ericaceae pollen, and nor was it reported at Langebaanweg (Coetzee and Rogers, 1982; Cole

521   and Roberts, 1996). It has however been identified in the Noordhoek borehole where it is

522   becomes progressively more abundant, along with the appearance of Asteraceae pollen in

523   the (assumed) Late Miocene to Pliocene (Coetzee 1983). Ericaceae is also found in the

524   Pliocene Varswater Formation assemblages (Scott, 1995). Asteraceae pollen is found at

525   Makhulu, suggesting potential correspondence with the Noordhoek and the Langebaanweg

526   sites. The Makhulu lignite therefore displays some commonalities with the Langebaanweg

527   pollen assemblages (palm, *Podocarpus*-type, Poaceae, Cyperaceae, Asteraceae, *Cliffortia*-

528   type, Anacardiaceae [*Rhus*-type]), and the lower parts of the Noordhoek record from which

529 a similar age, broadly equivalent to the middle Miocene, may be inferred. There are,

530 however, differences and the significant geographic separation of these regions should be

531 borne in mind. Such an age association is not inconsistent with the geomorphic evidence or

532 isotopic evidence at Makhulu. If the leaf wax stable isotope data are indeed influenced by a

533 significant C_4 vegetation contribution, an age more akin to the Late Miocene or younger

534 might be inferred for Makhulu.

535   A Miocene to Pliocene age range inferred for the Makhulu lignite places its

536 deposition within a key phase of the evolution and diversification of the Cape Flora, a period

537 that apparently records a major shift in the ecology of the Western Cape; *viz*, the demise of

538 the palms and tropical-affinity vegetation (Coetzee, 1983) and the diversification of many

539 succulent Karoo and *fynbos* plant lineages (Richardson et al., 2001). A major change around

540 the Late Miocene to Pliocene has been considered indicative of the progressive aridification

541 the Western Cape, which probably related to the ongoing expansion of Antarctic ice

542 (Coetzee, 1983; 1986; Zachos et al., 2001). This situation was also intimately related to the

543 intensification of the Benguela upwelling system (Marlow et al., 2000), which would have

544 reinforced summer atmospheric stability. It is difficult to assess when and how this would

545 have affected the southern Cape/Knysna region, which even today experiences distinctly

546 different climatic conditions to the Cape Town area. A potential C_4 signal in the *n*-alkane

547 stable isotopes implies, to some extent, conditions akin to the contemporary summer

548 rainfall regions of southern Africa (Vogel et al., 1978), and a response to late Neogene

549 reductions in atmospheric pCO$_2$ (Hopley et al., 2007). Given the pollen data presented here,

550 vegetation of a tropical affinity may have been restricted to the vicinity of wetlands (a 'palm

551 swamp' environment). In conjunction with evidence for an inferred absence of C_4 vegetation

552   on the west coast (Langebaanweg) area during the early Pliocene (Franz-Odendaal et al.,

553   2002) it is probable that distinct vegetation communities in the west coast and southern

554   Cape regions (and most likely contrasting climates) were established during this Late

555   Neogene climatic/ecological re-organisation.

556

557   **Conclusions**

558   The lignitic sediments exposed at Makhulu Quarry provide a new window on

559   Neogene palaeoenvironments of the southern Cape coastline. Analyses using the ITL

560   technique provide a revised minimum age of > 1.7 Ma for the Makhulu coversands,

561   suggesting a pre-Quaternary emplacement of the sands and lignite. Additional age

562   constraints on the lignite are provided by the compound specific $\delta^{13}C$ data, which imply a

563   potential presence of C_4 vegetation in the regional environment. The organic geochemistry

564   of the lignite is dominated by biomarkers derived from terrestrial plants, with no significant

565   evidence for a marine organic matter contribution. The pollen assemblage is dominated by

566   palms, as well as a riparian vegetation suite that probably surrounded the immediate

567   wetland site. A 'palm swamp' setting surrounded by vegetation comprising a mix of shrubs

568   and grasses and some arboreal species (e.g. *Podocarpus* sp.) is inferred. These data show

569   marked contrasts with some previous descriptions of palynology of the Knysna Formation,

570   but show some commonalities with pollen assemblages found in the Miocene Elandsfontein

571   Formation in the Western Cape. From this, a probable age range between the Miocene and

572   1.7 Ma is therefore proposed for the Makhulu lignite, which might be further refined to a

573   post late Miocene age should it prove possible to demonstrate that the *n*-alkane $\delta^{13}C$ signal

574   is dominated by a C_4 leaf wax contribution.

575

Acknowledgements

584

References

586 Aitken, M. J. (1985) *Thermoluminescence dating*. Academic Press, London and New York.

587 Banerjee, D., Hildebrand, A.N., Murray-Wallace, C.V., Bourman, R.P., Brooke, B.P. and Blair,
588   M. (2003) New quartz SAR-OSL ages from the stranded beach dune sequence in
589   south-east South Australia. *Quaternary Science Reviews,* **22**, 1019-1025.

590 Bateman, M.D., Holmes, P.J., Carr, A.S., Horton, B.P. and Jaiswal, M.K. (2004) Aeolianite and
591   barrier dune construction spanning the last two glacial–interglacial cycles from the
592   southern Cape coast, South Africa. *Quaternary Science Reviews,* **23**, 1681-1698.

593 Bechtel, A., Sachsenhofer, R.F., Kolcon, I., Gratzer, R., Otto, A. and Püttmann, W. (2002)
594   Organic geochemistry of the lower Miocene Oberdorf lignite (Styrian Basin, Austria):
595   its relation to peterology, palynology and the palaeoenvironment. *International*
596   *Journal of Coal Geology,* **51**, 31-57

597 Bechtel, A., Sachsenhofer, R.F., Markic, M., Gratzer, R., Lücke, A. and Püttmann, W. (2003)
598   Paleoenvironmental implications from biomarker and stable isotope investigations
599   on the Pliocene Velenje lignite seam (Slovenia). *Organic Geochemistry,* **34**, 1277-
600   1298.

601 Berrío, J.C., Hooghiemstra, H., Behling, H., Botero P., and Van der Borg, W. (2002)
602   Environmental history of the western Colombian savannas of the Llanos Orientales
603   since the Middle Holocene from Laguna Mozambique and Chenevo: a transect
604   synthesis. *The Holocene*, **12**, 35-48.

605 Besnard, G., Muasya, A.M., Russier, F., Roalson, E.H., Salamin, N. and Christin, P.A. (2009)
606   Phylogenomics of C_4 photosynthesis in sedges (Cyperaceae): multiple appearances
607   and genetic convergence. *Molecular Biology and Evolution*, **26**, 1909-19.

608 Bi, X., Sheng, G., Lui, X., Li, C. and Fu, J. (2005) Molecular and carbon and hydrogen isotopic
609   composition of *n*-alkanes in plant leaf waxes. *Organic Geochemistry,* **36**, 1405-1417.

610 Blokker, P., Schouten, S., Van den Ende, H., De Leeuw, J.W., Hatcher, P.G. and Sinninghe
611   Damsté, J.S. (1998) Chemical structure of algaenans from the fresh water algae
612   *Tetraedron minimum*, *Scenedesmus communis* and *Pediastrum boryanum*. *Organic*
613   *Geochemistry,* **29**, 1453-1468

614 Boom, A., Marchant, R., Hooghiemstra, H., and Sinninghe-Damsté, J.S. (2002) CO_2 and
615   temperature-controlled altitudinal shifts of C_4 and C_3 dominated grasslands allow
616   reconstruction of palaeo-atmospheric pCO$_2$. *Palaeogeography Palaeoclimatology*
617   *Palaeoecology,* **177**,151-168.

618 Boom, A., Sinninghe-Damsté, J.S., and de Leeuw, J.W. (2005) Cutan, a common aliphatic
619   biopolymer in cuticles of drought-adapted plants. *Organic Geochemistry,* **36**, 595–
620   601.

621 Buylaert, J.P., Murray, A.S., Huot, S., Vriend, M.G.A., Vandenberghe, D., De Corte, F. and Van
622   den haute, P. (2006) A comparison of quartz OSL and isothermal TL measurements
623   on Chinese loess. *Radiation Protection Dosimetry,* **119**, 474-478.

624 Butzer, K.W., Helgren, D.M. (1972) Late Cenozoic evolution of the Cape coast between
625   Knysna and Cape St Francis, South Africa. *Quaternary Research,* **2**, 143-169.

626 Cerling, T., Wang, Y. and Quade, J. (1993) Expansion of C_4 ecosystems as indicator of global
627   ecological change in the Late Miocene. *Nature,* **361**, 344-345.

628 Choi, J.H., Murray, A.S., Cheong, C.-S., Hong, D.G., and Chang, H.W. (2006) Estimation of
629   equivalent dose using quartz isothermal TL and the SAR procedure. *Quaternary*
630   *Geochronology,* **1**, 101-108.

631 Coetzee, J.A. (1983) Intimations on the Tertiary vegetation of southern Africa. *Bothalia,* **14**,
632   345-354.

633 Coetzee, J.A. (1986) Palynological evidence for major vegetation and climatic-change in the
634   Miocene and Pliocene of the southwestern Cape. *South African Journal of Science,*
635   **82**, 71-72

636 Coetzee, J.A. and Rogers, J. (1982) Palynological and lithological evidence for the Miocene
637   Palaeoenvironment in the Saldanha region, South Africa. *Palaeogeography*
638   *Palaeoclimatology Palaeoecology,* **38**, 71-85

639 Coetzee, J.A., Scholtz, A. and Deacon, H.J. (1983) Palynological studies and vegetation
640   history of the fynbos. In Deacon, H.J et al. *Fynbos Palaeoecology: a preliminary*
641   *synthesis*, CSIR Report 75, p156-173.

642 Cole, D.I. and Roberts, D.L. (1996) Lignite from the western coastal plain of South Africa.
643   *Journal of African Earth Sciences,* **23,** 95-117

644 Collister, J.W., Rieley, G., Stern, B., Eglinton, G. and Fry, B. (1994) Compound-specific δ^{13}C
645   analyses of leaf lipids from plants with differing carbon dioxide metabolisms. *Organic*
646   *Geochemistry,* **21**, 619-627.

647 Conte, M.H. and Weber, J.C. (2002) Plant biomarkers in aerosols record isotopic
648   discrimination of terrestrial photosynthesis. *Nature* **417**, 639-641

649 Du Toit, A.L. (1956) *The Geology of South Africa* (Third Edition). Oliver and Boyd, Edinburgh.

650 Eglinton, G. and Hamilton, R. (1967) Leaf epicuticular waxes. *Science,* **156**, 1322-1335

651 Eglinton, T.I. and Eglinton, G. (2008) Molecular proxies for paleoclimatology. *Earth and*
652   *Planetary Science Letters,* **275**, 1-16

31

653   Ficken, K.J., Li, B., Swain, D.L. and Eglinton, G. (2000) An *n*-alkane proxy for the sedimentary
654   input of submerged/floating freshwater aquatic macrophytes. *Organic Geochemistry,*
655   **31**, 745-749

656   Franklin, A.D. (1997) On the interaction between the rapidly and slowly bleaching peaks in
657   the TL glow curves of quartz. *Journal of Luminescence,* **75**, 71-76

658   Franz-Odendaal, T.A., Lee-thorp, J.A. and Chinsamy, A. (2002) Evidence for the lack of C_4
659   grassland expansions during the Early Pliocene at Langebaanweg, South Africa.
660   *Paleobiology,* **28**, 378-388

661   Freeman, K.H. and Calarusso, L.A. (2001) Molecular and isotopic records of C_4 grassland
662   expansion in the Late Miocene. *Geochimica et Cosmochimica Acta,* **65**, 1439-1454.

663   Galbraith, R.F., Roberts, R.G., Laslett, G.M., Yoshida, H. and Olley, J.M. (1999). Optical dating
664   of single and multiple grains of quartz from Jimnium rock shelter, northern Australia,
665   Part 1, experimental design and statistical models. *Archaeometry,* **41**, 229-364

666   Gupta, N.S., Michels, R., Briggs, D.E.G., Collinson, M.E., Evershed, R.P. and Pancost, R.D.
667   (2007) Experimental evidence for the formation of geomacromolecules from plant
668   leaf lipids. *Organic Geochemistry,* **38**, 28-36

669   Harley, M.M. and Baker, W.J. (2001) Pollen aperture morphology in Arecaceae: application
670   within phylogenetic analyses, and a summary of the fossil record of palm like pollen.
671   *Grana,* **40**, 45-77.

672   Haq, B.V., Hardenbol, J. and Vail, P.R. (1987) Chronology of fluctuating sea levels since the
673   Triassic. *Science,* **235**, 1156-1167.

674   Helgren, D.M. and Butzer, K.W. 1977. Paleosols of the southern Cape coast, South Africa:
675   Implications for laterite definition, genesis and age. *Geographical Review,* **67**, 430-
676   445.

677   Holmes, P.J., Bateman, M.D., Carr, A.S. and Marker, M.E. (2007) The place of the aeolian
678   coversands in the geomorphic evolution of the southern Cape coast, South Africa.
679   *South African Journal of Geology*, **110**, 127-138

680   Hopley, P.J., Marshall, J.D., Weeden, G.P., Latham, A.G., Herries, A.I.R. and Kuykendall, K.L.
681   (2007) Orbital forcing and the spread of C_4 grasses in the late Neogene: stable
682   isotope evidence from South African speleothems. *Journal of Human Evolution,* **53**,
683   620-634.

684   Huot, S., Buylaert, J.P. and Murray A.S. (2006) Isothermal thermoluminescence signals from
685   quartz. *Radiation Measurements,* **41**, 796-802.

686   Jacobs, E.O. (1992) *Lithostratigraphy of the Knysna Formation*. South African Committee for
687   Stratigraphy Lithostratigraphic Series 17, Government Printer, Pretoria.

688   Jain, M., Duller, G.A.T. and Wintle, A.G. (2007) Dose response, thermal stability and optical
689   bleaching of the 310°C isothermal TL signal in quartz. *Radiation Measurements,* **42**,
690   1285-1293.

691   John, C.M., Karner, G.D. and Mutti, M. (2004) $\delta^{18}O$ and Marion Plateau backstripping:
692   Combining two approaches to constrain late middle Miocene eustatic amplitude.
693   *Geology*, **32**, 829-832

694   Linder, H.P. (2003) The radiation of the Cape flora, southern Africa. *Biological Reviews of the*
695   *Cambridge Philosophical Society*, **78**, 597–638.

696   Le Roux, F.G. (1990) Palaeontological correlation of Cenozoic marine deposits of the
697   southeastern, southern and western coasts, Cape Province. *South African Journal of*
698   *Geology,* **93**, 514-518.

699   Logan, G.A., Boon, J.J. and Eglinton G. (1993) Structural biopolymer preservation in Miocene
700   leaf fossils from the Clarkia site, northern Idaho. *Proceedings of the National*
701   *Academy of Sciences of the United States of America,* **90**, 2246-2250.

702   Ledru, M.P. (2001) Late Holocene rainforest disturbance in French Guiana. *Review of*
703   *Palaeobotany and Palynology,* **115**, 161-176

704   Marker, M.E. and Holmes, P.J. (2002) The distribution and environmental implications of
705   coversand depsots in the southern Cape. *South African Journal of Geology,* **105**, 135-
706   146.

707   Marker, M.E. and Holmes, P.J. (2005) Landscape evolution and landscape sensitivity: the
708   case of the southern Cape. *South African Journal of Science,* **101**, 53-60.

709   Marlow, J.R., Lange, C.B., Wefer, G. and Rosell-Melé, A. (2000) Upwelling intensification as
710   part of the Pliocene-Pleistocene climate transition. *Science,* **290**, 2288-2291.

711   Martin A.R.H (1968) Pollen analysis of Groenvlei lake catchments, Knysna. *Review of
712   Palaeobotany and Palynology,* **7**, 107-144.

713   Meyers, P.A. and Lallier-Vergés, E. (1999) Lacustrine sedimentary organic matter records of
714   Late Quaternary palaeoclimates. *Journal of Paleolimnology,* **21**, 345-372.

715   Miller, K.G., Kominz, M.A. Browning, J.V., Wright, J.D., Mountain, G.S., Katz, M.E., Sugarman,
716   P.J., Cramer, B.S., Christie-Blick, N. and Pekar, S.F. (2005) The Phanerozoic record of
717   global sea-level change. *Science*, **310**, 1293 - 1298

718   Murray, A.S., and Wintle, A.G. (2000) Luminescence dating of quartz using an improved
719   single-aliquot regenerative-dose protocol. *Radiation Measurements,* **32**, 57-73.

720   Nip, M., Tegelaar, E.W., de Leeuw J.W. and Schenck, P.A. (1986) A new non-saponifiable
721   highly aliphatic and resistant biopolymer in plant cuticles. *Naturwissenschaften,* **73**,
722   579–585.

723   Otto, A., Simoniet, B.R.T. and Rember, W.C. (2005) Conifer and angiosperm biomarkers in
724   clay sediments and fossil plants from the Miocene Clarkia Formation, Idaho, USA.
725   *Organic Geochemistry,* **36**, 907-922.

726   Pancost, R.D. and Boot, C.S. (2004) The palaeoclimatic utility of terrestrial biomarkers in
727   marine sediments. *Marine Chemistry,* **92**, 239-261.

728   Pancost, R.D., Steart, D.S., Handley, L., Collinson, M.E., Hooker, J.J., Scott, A.C., Grassineau,
729   N.V. and Glasspool, I.J. (2007) Increased terrestrial methane cycling at the
730   Palaeocene-Eocene thermal maximum. *Nature,* **449**, 332-335

731   Partridge, A.D. (1978) Palynology of the late Tertiary sequence at Site 365, Leg 40. *Deep Sea
732   Drilling Project Initial Reports,* **40**, 953–961.

733   Partridge, T.C. and Maud, R.R. (1987) Geomorphic evolution of southern Africa since the
734   Mesozoic. *South African Journal of Geology,* **90**, 179-208.

735   Phillips, J.F.V. (1927) Fossil *Widdringtonia* in lignite of the Knysna Series, with a note on
736   fossil leaves of several other species. *South African Journal of Science,* **24**, 188-197

737   Richardson, J.E., Weitz, F.M., Fay, M.F., Cronk, Q.C.B., Linder, H.P., Reeves, G. and Chase,
738   M.W. (2001) Rapid and recent origin of species richness in the Cape flora of South
739   Africa. *Nature,* **412**, 181-183.

740   Roberts, D.L. and Brink, J.S. (2002) Dating and correlation of Neogene coastal deposits in the
741   Western Cape (South Africa): implications for Neotectonism. *South African Journal of*
742   *Geology,* **105**, 337-352

743   Rommerskirchen, F., Eglinton, G., Dupont, L., Güntner, U., Wenzel C. and Rullkötter, J.
744   (2003) A north to south transect of Holocene southeast Atlantic continental margin
745   sediments: relationship between aerosol transport and compound-specific δ^{13}C plant
746   biomarker and pollen records. *Geochemistry, Geophysics, Geosystems* **4** (12) 1101.

747   Scott, L. (1982) Late Quaternary fossil pollen grains from the Transvaal, South Africa. *Review*
748   *of Palaeobotany and Palynology* 36, 241-278

749   Scott, L (1995) Pollen evidence for vegetational and climatic change in southern Africa
750   during the Neogene and Quaternary. In: Vrba, E.S., Denton, G.H., Partridge, T.C. and
751   Burckle, L.H. (eds). *Palaeoclimate and evolution with emphasis on human origins*.
752   Yale University Press, pp 65-76.

753   Ségelan, L., Lee-Thorp, J.A. and Cerling, T. (2007) Timing of C_4 grass expansion across sub-
754   Saharan Africa. *Journal of Human Evolution,* **53**, 549-559.

755   Skvarla,J.J., DeVore, M.L., and Chissoe, WF. (2005) Lophate sculpturing of Vernonieae
756   (Compositae) pollen. *Review of Palaeobotany and Palynology,* 133, 51-68

757   Stefanovaa, M., Markovab, K., Marinova, S. and Simoneit, B.R.T. (2005) Molecular indicators
758   for coal-forming vegetation of the Miocene Chukurovo lignite, Bulgaria. *Fuel,* **84**,
759   1830-1838.

760   Street-Perrott, F.A., Ficken, K.J., Huang, Y. and Eglinton, G. (2004) Late Quaternary changes
761   in carbon cycling on Mt. Kenya, East Africa: an overview of the $\delta^{13}C$ record in
762   lacustrine organic matter. *Quaternary Science Reviews,* **23**, 861-879.

763   Stock, W.D., Chuba, D.K. and Verboom, G.A. (2004) Distribution of South African C_3 and C_4
764   species of Cyperaceae in relation to climate and phylogeny. *Austral Ecology*, **29**, 313–
765   319

766   Thiergart, F., Frantz, U. and Raukopf, K. (1963) Palynologische untersuchungen von
767   Tertiärkohlen und einer oberflächen-probe nahe Knysna, Südafrika. *Advancing*
768   *Frontiers in Plant Science,* **4**, 151-178.

769   Thwaites, R.N. and Jacobs, E.O. (1987) The Knysna Lignites: a review of their position within
770   the geomorphological development of the southern Cape Province, South Africa.
771   *South African Journal of Geology,* **90**, 137-146

772   Tipple, B.J. and Pagani, M. (2007) The early origins of terrestrial C_4 photosynthesis. *Annual*
773   *Reviews of Earth and Planetary Science,* **35**, 435-461

774   Tripati, A.K., Roberts, C.D. and Eagle, R.A. (2009) Coupling of CO_2 and ice sheet stability over
775   major climate transitions of the last 20 million years. *Science*, **326**, 1394 - 1397

776   Vandenberghe, D.A.G., Jain, M. and Murray, A.S. (2009) Equivalent dose determination
777   using a quartz isothermal TL signal. *Radiation Measurements,* **44**, 439-444.

778   Van Zinderen Bakker, E.M. (1984) Palynological evidence for Late Cenozoic arid conditions
779   along the Namibia coast from Hole 532 and 530A, Leg 75, Deep Sea Drilling Project.
780   *Deep Sea Drilling Project Initial Reports,* **75**, 763-768

781   Vogel, J.C., Fuls, A. and Ellis, R.P. (1978) The geographical distribution of Kranz grasses in
782   South Africa*. South African Journal of Science,* **74**, 209-215.

783   Volkman, J.K., Revill, A.T., Holdsworth, D.G. and Fredericks, D. (2008) Organic matter
784   sources in an enclosed coastal inlet assessed using lipid biomarkers and stable
785   isotopes. *Organic Geochemistry,* **39**, 689-710

786 Wintle, A.G. and Murray, A.S. (2006) A review of quartz optically stimulated luminescence
787   characteristics and their relevance in single-aliquot regeneration dating protocols.
788   *Radiation Measurements,* **41**, 369-391

789 Yang, H., Huang, Y., Leng, Q., Le Page B.A. and Williams, C.J. (2005) Biomolecular
790   preservation of Tertiary *Metasequoia* fossil *Lagerstätten* revealed by comparative
791   pyrolysis analysis. *Review of Palaeobotany and Palynology,* **134**, 237–256.

792 Zachos, J.C., Pagani, M., Sloan, L., Thomas, E. and Billups, K. (2001) Trends, rhythms, and
793   abberations in global climate 65 Ma to present. *Science,* **292**, 686–693.

794

795 **Table Captions**

796 **Table 1:** Details of the SAR ITL protocol used in this study (following Choi et al. 2006). All heating was
797 carried out at 2°C s^{-1}. *Di is 0 Gy in the first cycle (i = 0) when the natural dose is measured. Preheat
798 T and ITL T were determined experimentally (see text).

Stage	Treatment	Record
1	Administer regeneration dose D_i*	-
2	Preheat for 10 s at T°C	-
3	ITL at T°C for 500 s	ITL L_i
4	Give fixed test dose D_t	-
5	Preheat for 10 s at T°C	-
6	ITL at T°C for 500 s	ITL T_i
7	Repeat steps 1-6	-

799

800 **Table 2:** Details of the OSL age determinations including dose rate data, equivalent doses and
801 resulting ages
802 * D_e values used to calculate a minimum age excludes aliquots which were saturated and as such represents a
803 conservative estimation of minimum palaeodose
804 # published in Holmes et al (2007)
805 $ determined using beta counting
806 ~Derived using the 'central age model' (Galbraith et al., 1999) and reported with 1 standard error

Sample Details			Dosimetry Data			OSL Data		ITL Data	
Site	Lab code	Depth (m)	Cosmic dose (µGy a^{-1})	Water content (%)	Total dose rate (µGy a^{-1})	Average D_e~ (Gy)	Age (ma)	Average D_e ~ (Gy)	Age (Ma)
Barrington Road	Shfd08191	3	170 ± 8	4.2	804 ± 66$^\$$	232 ± 6	**0.29 ± 0.02**	291 ± 15	**0.36 ± 0.04**
Makhulu Quarry	Shfd04287	1.6	174 ± 9	4.8	475 ± 20$^\#$	248 ± 11*	**>0.52$^\#$**	806 ± 58*	**>1.70**

807   **Table 3:** Bulk carbon and nitrogen contents, and δ^{13}C of the sampled lignite, along with *n*-alkane
808   derived indices from the apolar solvent extraction.

Total organic carbon (%)	38.5
$\delta^{13}C_{TOC}$ (‰)	-26.6
Total Nitrogen (%)	0.8
TOC/TN	45
***n*-alkane Carbon Preference Index (CPI: C_{25}-C_{34})**	4.57
***n*-alkane average chain length (C_{23}-C_{33})**	27.9
P_{aq} (Ficken et al, 2000)	0.42

809

810   **Table 4**: Compound specific δ^{13}C data. Weighted mean *n*-alkane δ^{13}C is weighted by relative peak
811   area.

Compound	Concentration ($\mu g\ g^{-1}$)	δ^{13}C (‰)
C_{25} alkane	11.3	-25.6
C_{26} alkane	2.57	-26.6
C_{27} alkane	8.98	-25.2
C_{28} alkane	2.09	-25.8
C_{29} alkane	8.46	-28.1
C_{31} alkane	13.9	-28.0
C_{33} alkane	2.06	-27.3
Weighted mean *n*-alkane		-27.0
Des-A-Lupane	16.0	-24.4
17β21β 30normoretane	1.99	-25.2
17β 21β Homohopane	0.77	-20.6

812

813

814

815 **Table 5**: Comparative table showing the Makhulu pollen data in relation previous reports of the
816 Knysna Formation and Western Cape sites reported by Coetzee and Rogers (1982) and Cole and
817 Roberts (1996) *Only pollen types listed in paper footnotes and/or referred to in Scott (1995) are
818 shown here.

Pollen type	Knysna Formation					West Coast (Elandsfontein Formation: Miocene)	
	Makhulu quarry	Coetzee et al. (1983)	Thiergart et al. (1963)	Helgren and Butzer (1977)*		Cole and Roberts (1996)	Coetzee and Rogers (1982)
Palm (Arecaceae)	Y (37%)	?		Y			Y
Cupressaceae							Y
Podocarpus-sp	Y (3.7%)	Y	Y				Y
Sapotaceae	Y (6.6%)						
Symphonia-type	Y (5.0%)						
Casuarinaceae		Y					Y
Cunonia?-type	Y (1.2%)						
Oleaceae			Y				Y
Ulmaceae							Y
Poaceae	Y (4.6%)			Y (rare)		Y	Y
Euphorbiaceae	? (0.4%)		Y?				Y
Asteraceae	Y (2.9%)					Y	Y
Anacardiaceae	Y (2.5%)		Y				Y
Rhus-type	Y (0.4%)	Y	Y			Y	?
Rubiaceae	Y (0.4%)	?					Y
Anthospermum-type	Y (0.4%)	?				Y	?
Myricaceae	Y (1.2%)						
Cliffortia-type	Y (0.4%)	Y				Y	Y
Cyperaceae	Y (6.7%)		Y			Y	
Ericaceae							
Proteaceae	? (0.4%)	Y	Y	Y		Y	Y
Restionaceae		Y	Y			Y	
Thymelaceae							?
Myrtaceae		Y					

819